

Transcriptional and Proteomic Analysis of the *Aspergillus fumigatus* Δ *prtT* Protease-Deficient Mutant

Shelly Hagag¹, Paula Kubitschek-Barreira², Gabriela W. P. Neves², David Amar³, William Nierman⁴, Itamar Shalit⁵, Ron Shamir³, Leila Lopes-Bezerra², Nir Osherov^{1*}

1 Department of Clinical Microbiology and Immunology, Sackler School of Medicine Ramat-Aviv, Tel-Aviv, Israel, **2** Department of Cellular Biology, The Roberto Alcantara Gomes Institute of Biology, University of Estado Rio de Janeiro, Brazil, **3** Department of Computer Science, Tel-Aviv University, Ramat-Aviv, Tel-Aviv, Israel, **4** The J. Craig Venter Institute, Rockville, Maryland, United States of America, **5** Sackler School of Medicine, Ramat Aviv, Tel-Aviv, Israel

Abstract

Aspergillus fumigatus is the most common opportunistic mold pathogen of humans, infecting immunocompromised patients. The fungus invades the lungs and other organs, causing severe damage. Penetration of the pulmonary epithelium is a key step in the infectious process. *A. fumigatus* produces extracellular proteases to degrade the host structural barriers. The *A. fumigatus* transcription factor PrtT controls the expression of multiple secreted proteases. PrtT shows similarity to the fungal Gal4-type Zn(2)-Cys(6) DNA-binding domain of several transcription factors. In this work, we further investigate the function of this transcription factor by performing a transcriptional and a proteomic analysis of the Δ *prtT* mutant. Unexpectedly, microarray analysis revealed that in addition to the expected decrease in protease expression, expression of genes involved in iron uptake and ergosterol synthesis was dramatically decreased in the Δ *prtT* mutant. A second finding of interest is that deletion of *prtT* resulted in the upregulation of four secondary metabolite clusters, including genes for the biosynthesis of toxic pseurotin A. Proteomic analysis identified reduced levels of three secreted proteases (ALP1 protease, TppA, AFUA_2G01250) and increased levels of three secreted polysaccharide-degrading enzymes in the Δ *prtT* mutant possibly in response to its inability to derive sufficient nourishment from protein breakdown. This report highlights the complexity of gene regulation by PrtT, and suggests a potential novel link between the regulation of protease secretion and the control of iron uptake, ergosterol biosynthesis and secondary metabolite production in *A. fumigatus*.

Citation: Hagag S, Kubitschek-Barreira P, Neves GWP, Amar D, Nierman W, et al. (2012) Transcriptional and Proteomic Analysis of the *Aspergillus fumigatus* Δ *prtT* Protease-Deficient Mutant. PLoS ONE 7(4): e33604. doi:10.1371/journal.pone.0033604

Editor: Robert A. Cramer, Montana State University, United States of America

Received: December 6, 2011; **Accepted:** February 13, 2012; **Published:** April 13, 2012

Copyright: © 2012 Hagag et al. This is an open-access article distributed under the terms of the Creative Commons Attribution License, which permits unrestricted use, distribution, and reproduction in any medium, provided the original author and source are credited.

Funding: This work was funded by an Israel Academy of Sciences grant (186/09) and an Israel Ministry of Health grant (3–5201) to NO. The funders had no role in study design, data collection and analysis, decision to publish, or preparation of the manuscript.

Competing Interests: The authors have declared that no competing interests exist.

* E-mail: nosherov@post.tau.ac.il

Introduction

Aspergillus fumigatus is a saprophytic mold which grows naturally on degrading organic materials. Its small-sized conidia can easily reach the pulmonary alveoli by inhalation and cause a variety of pathological conditions [1]. Invasive Pulmonary Aspergillosis (IPA) is considered the most severe condition, threatening the lives of immunocompromised patients [2]. Infection can occur when the compromised immune system fails to eradicate the conidia from the lungs allowing germination, colonization and eventually penetration of the fungus through the pulmonary epithelium into the blood stream [3].

The ability of *A. fumigatus* to infect and persist inside the body has been attributed to an array of factors including: conidial pigmentation, secreted toxins, surface and cell-wall components, the ability to endure hypoxia, an efficient iron-uptake system and the secretion of proteases [4,5]. In human A549 alveolar epithelial cells, culture filtrates (CFs) of *A. fumigatus* have been shown to disrupt the actin cytoskeleton, induce the production of proinflammatory cytokines and activate NF κ B signaling. The addition of serine protease inhibitors to the secreted CF prevents these cellular events, suggesting that they are directly dependent on secreted fungal proteases [6,7]. Recently, it has been shown that *A.*

fumigatus-secreted proteases degrade complement proteins, which may serve as a mechanism for partially evading the immune defenses [8,9].

Studying the process by which protease production is modulated led to the characterization of a proteolysis-deficient strain of *A. fumigatus* in which the transcription factor PrtT, a positive regulator of secreted proteases, is disrupted. The Δ *prtT* mutant exhibits a reduction in the transcription of secreted proteases and subsequently, reduced proteolytic activity of the CF. Δ *prtT* CF showed reduced killing of A549 lung alveolar cells and erythrocyte lysis [10,11,12]. However, the virulence of the Δ *prtT* strain was not attenuated in a murine model of IPA. The reconstituted *prtT* strain showed WT features under all examined conditions, validating that the phenotype of the Δ *prtT* mutant is the result of disruption of the *prtT* gene alone.

To better understand the role of PrtT in the control of gene expression and its effect on the secretome, we performed a combination microarray- and proteomics-based secretome analysis of the Δ *prtT* mutant. Microarray analysis has been used previously in *A. fumigatus* to identify the putative downstream targets of several transcription factors, including CrzA, SrbA, LaeA, SreA, HapX, AcuM, BrlA and StuA [13,14,15,16,17,18,19]. Proteomic analysis of *A. fumigatus* mutants

in which key transcription factors are deleted has only been performed for *AfYap1*, involved in defense against reactive oxygen species [20].

Here we describe novel and unexpected findings showing that in addition to activating the expression of key secreted proteases, PrtT is also involved in regulating the transcription of genes involved in iron uptake, ergosterol biosynthesis and secondary metabolite biosynthesis. At the secretome level, deletion of PrtT not only reduces the secretion of key proteases but also alters the expression pattern of other apparently unrelated secreted proteins. Our work highlights the complexity of transcriptional regulation by PrtT.

Materials and Methods

Strains and culture conditions

A. fumigatus strain Af293, originally isolated at autopsy from a patient with IPA, and the *A. fumigatus* *prtT* disruption mutant (*ΔprtT*) derived from Af293, were used throughout this study [11]. Generation of the *AsidA* mutant strain was as described by Schrettl et al. [21]. For continuous growth, the different *A. fumigatus* strains were grown on YAG medium, which consists of 0.5% (wt/vol) yeast extract, 1% (wt/vol) glucose, and 10 mM MgCl₂, supplemented with trace elements, vitamins, and 1.5% (wt/vol) agar when needed [22]. Skim milk (SM) medium consisted of 1% (wt/vol) glucose, 1% or 0.1% (wt/vol) SM (Difco, Livonia, MI), 0.1% (wt/vol) Casamino Acids (Difco), 7 mM KCl, 2 mM MgSO₄ and 50 mM Na₂HPO₄-NaH₂PO₄ buffer (pH 5.3), supplemented with vitamins, trace elements (including 4 μM FeCl₂), and 1.5% agar when needed [23]. Where indicated, ferrozine (Sigma Aldrich Corp., St Louis, MO) was added to the media 24 h prior to use. Conidia were harvested in PBS and counted with a hemocytometer.

RNA extraction

Total RNA was isolated from each strain using the QIAGEN RNeasy Plant Kit (QIAGEN Inc. Valencia, CA) following the protocol for filamentous fungi. The RNA was digested with Turbo-DNase (Ambion, Austin, TX) according to the manufacturer's instructions.

Sample preparation for microarray analysis

1×10⁷ conidia (WT or *ΔprtT* strains) were grown in 50 ml of 1% SM medium for 24 h at 37°C in an orbital incubator at 180 rpm. The mycelium was harvested using miracloth (Calbiochem, San-Diego, CA) and subsequently freeze-dried. Total RNA from three independent biological repeats was extracted, assessed for purity by the Agilent Bioanalyzer and shipped in isopropanol to the Nierman laboratory (JCVI) for microarray analysis.

Microarray Analysis

Transcriptional profiling in this study was achieved using the *A. fumigatus* (Af293) DNA amplicon array containing 9516 genes as described previously [24]. The expression profiles were analyzed using EXPANDER, a general microarray analysis software [25]. EXPANDER supports all analysis steps, including normalization and filtering, gene clustering and differential expression analysis, and various statistical tests for gene group analysis including functional enrichment and transcription factor binding site enrichment. Differential genes were defined as genes whose expression level was altered by at least twofold, in at least two out of the three repeats. This criterion yielded a group of 229 upregulated genes and a group of 199 downregulated genes (Supporting Information S1). For each of these groups GO

functional enrichment was evaluated using TANGO (FDR <0.05). Enrichment for other gene functional classes such as secreted proteases [26], iron uptake [14,27] and ergosterol biosynthesis [24] was performed using a hyper geometric test (Bonferroni corrected <0.05). Microarray datasets were deposited at Gene Accession Omnibus [28], accession numbers GSE33254).

Quantitative real-time (qRT)-PCR

Conidia were grown in SM medium and total RNA was prepared as described above. When indicated, ferrozine (Sigma) or voriconazole (Pfizer, NY, USA) was added to the media at a final concentration of 1 mM and 0.125 μg/ml (half MIC), respectively.

RNA concentration was assessed using a NanoDropTM 1000 Spectrophotometer (Thermo Scientific Inc. Barrington IL) and 1 μg was taken for the RT reaction using StrataScript Reverse Transcriptase (Stratagene; Cedar Creek, TX). Gene-specific primers for expression analysis are listed in Supporting Information S2, Table A. Whenever possible the primers were located on the junction between exons or in different exons. As a standard control, reactions using primers specific for the β-tubulin gene (AFUA_1G10910) of *A. fumigatus* were performed. qRT-PCR was performed on an ABI Prism PCR-HT7900 using 500 nM primers and Power SYBR green PCR Master Mix (Life Technologies Inc. Carlsbad CA). All reactions were performed in triplicates, and the mixture included a negative no-template control.

Growth in iron-limited media

A. fumigatus wild-type (WT) and *ΔprtT* mutant strains were grown on 0.1% SM agar plates lacking iron and supplemented with different concentrations of the ferrous iron chelator, ferrozine. Conidia were point-inoculated on the agar using a toothpick dipped in PBS containing 1×10⁶ conidia/ml. Plates were incubated for 48 h at 37°C and the diameter of the colonies measured. In the positive control, the medium was supplemented with iron (8 μM FeCl₂).

Evaluation of siderophore production

A modification of the chrome azurol S (CAS) assay was used to detect siderophore production in *A. fumigatus* [29,30]. This assay is based on competition for iron between the ferric complex of an indicator dye, CAS, and a chelator or siderophore. The iron is removed from CAS by the siderophore, which has a higher affinity for iron (III). This reaction results in a color change of the CAS reagent (usually from blue to orange). Conidia were grown at a concentration of 1×10⁶ conidia/ml in 1 ml of 1% SM medium in 24-well plates for 48 h at 37°C. The 1% SM medium contained iron (FeCl₂ 8 μM) or no iron supplemented with the ferrous iron chelator ferrozine (1 mM). Culture supernatants were collected after 48 h and 100 μl was added to wells that were cut out of the CAS agar plates. Plates were incubated at 37°C for 4 h. The change in color or the presence of a halo around the well after incubation indicated siderophore production.

Sensitivity to voriconazole by agar dilution

A. fumigatus WT or *ΔprtT* mutant strains were grown on 1% SM agar plates supplemented with different concentrations of voriconazole. Conidia were point-inoculated on the agar using a toothpick dipped in PBS containing 1×10⁶ conidia/ml. Plates were incubated for 48 h at 37°C and the diameter of the colonies measured.

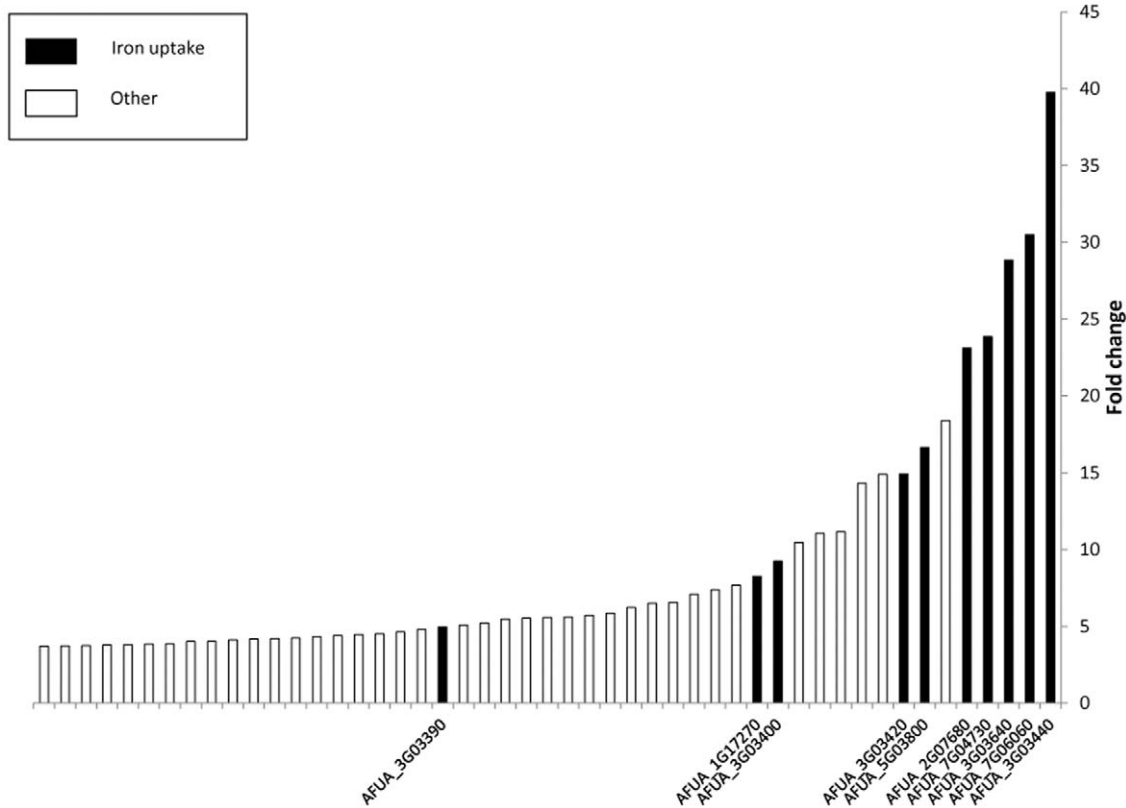


Figure 1. Top 50 downregulated genes plotted in ascending order by fold change. Black bars are the iron uptake genes, white bars are genes with various other annotations.
doi:10.1371/journal.pone.0033604.g001

Preparation of fungal CF for proteomics

A. fumigatus WT or *AprtT* mutant strains were grown at a concentration of 1×10^6 conidia/ml in flasks containing 250 ml SM medium. Fungal cultures were grown in an orbital incubator for 48 h at 37°C, 180 rpm. Samples were strained using miracloth and the CF collected. CFs were dialyzed at 4°C against DDW, using a Cellulose Membrane (Cellu-Sep T2/Nominal MWCO: 6,000 – 8,000) for 24 h and then freeze-dried.

SDS-PAGE

The secretome extracts of the WT and *AprtT* strains were first precipitated by 20% trichloroacetic acid/acetone (vol/vol), suspended in rehydration buffer (30 mM Tris, 7 M urea, 2 M thiourea, 4% wt/vol CHAPS) and protein concentration was determined either by the Bradford method or the BCA Protein Assay Kit (Thermo Scientific; Rockford, IL). Then, 10 µg of each secretome extract was separated by 12% SDS-polyacrylamide gel electrophoresis in a miniPROTEAN system (Bio-Rad laboratories Inc., Hercules CA). The 1D gels were stained with colloidal Coomassie [31] and gel pieces were excised for further protein identification.

DIGE 2D-gel electrophoresis

Protein abundance was compared between the WT and *AprtT* secretomes using four replicates for each experimental condition. Each sample was minimally labeled with CyDyes (Cy3 or Cy5) according to the manufacturer's instructions (GE Healthcare, Waukesha WI). An internal pool generated by equal amounts of all extracts was labeled with Cy2. The focusing was performed using

IPG strips (Immobiline DryStrip 3–11 NL, 18 cm), with the addition of 1,2% DeStreak and 1% IPG buffer 3–11 (GE Healthcare). Immobilized pH-gradient strips were reduced (1.5% wt/vol dithioerythritol) and alkylated (2.5% wt/vol iodoacetamide) in equilibration buffer (6 M urea, 50 mM Tris-HCl, pH 6.8, 30% glycerol, 2% SDS). Equilibrated strips were run on homogeneous 12% polyacrylamide gels using an Ettan DALTsix electrophoresis system with low-fluorescence glass plates (GE Healthcare). All gels, after image analysis (described below), were stained by colloidal Coomassie [31].

2D-DIGE image analysis

Protein spots were visualized by a Typhoon Trio variable mode Imager (GE Healthcare) using a resolution of 100 µm, and the quantification of protein expression was carried out with the DeCyder 7.0 software package (GE Healthcare). The Cy2 channel from each gel was used for normalization of the spot intensities. Inter-gel matching and statistical analysis were performed using DeCyder BVA (Biological Variance Analysis) module, and each comparison was filtered to find the spots having (a) P-value ≤ 0.05 and (b) greater than 1.5-fold change in expression between the groups. The Extended Data Analysis (EDA module) was used to perform the Principal Component Analysis (PCA) to identify underlying sources of variation [30].

In-gel digestion and protein identification

Spots of interest were manually excised from 2-DE gels. The gel pieces were destained, shrunk, vacuum-dried and the peptides digested according to [32]. After digestion the samples were spotted on a MALDI target plate (Applied Biosystems) and mixed

Table 1. Selected enriched downregulated gene classes in the *ΔprtT* mutant vs. WT¹.

Enriched class	Gene ID	Gene description	Fold change
Secreted proteases P=0.002	AFUA_4G11800	alkaline serine protease Alp1	-14.3
	AFUA_6G00310	serine carboxypeptidase (CpdS),	-3.6
	AFUA_7G04930	alkaline serine protease (PR1),	-2.5
	AFUA_2G17330	serine peptidase, family S28,	-2.2
	AFUA_8G07080	Elastinolytic metalloproteinase Mep	-2.1
Iron uptake P=1E-15	AFUA_3G03440	MFS family siderophore transporter, putative	-39.8
	AFUA_7G06060	siderochrome-iron transporter (Sit1), putative	-30.5
	AFUA_3G03640	siderochrome-iron transporter (MirB), putative	-28.8
	AFUA_7G04730	siderochrome-iron transporter, putative	-23.9
	AFUA_2G07680	L-ornithine N5-oxygenase SidA	-23.1
Sterol and Fatty Acid Biosynthesis P=0.001	AFUA_2G00320	sterol delta 5,6-desaturase,	-6.5
	AFUA_1G03150	c-14 sterol reductase	-4.2
	AFUA_4G06890 ²	14-alpha sterol demethylase Cyp51A, ERG11	-4.2
	AFUA_5G07780 ²	Squalene monooxygenase ERG1	-3.7
	AFUA_6G05140 ²	sterol delta 5,6-desaturase, ERG3	-2.9
Cellular ketone metabolic process P=0.001	AFUA_6G07720 ³	homogentisate 1,2-dioxygenase (HmgA), putative	-4.2
	AFUA_2G04220	phosphoenolpyruvate carboxykinase (ATP) (AcuF)	-4.0
	AFUA_4G06620	NADP-dependent malic enzyme (MaeA)	-3.5
	AFUA_2G08280 ³	proline oxidase (PrnD)	-3.5
	AFUA_5G04250 ³	fumarylacetoacetate hydrolase (FahA)	-3.3
Oxidoreductase activity P=0.008	AFUA_1G17180	pyridine nucleotide-disulphide oxidoreductase, putative	-7.7
	AFUA_5G03930	alcohol dehydrogenase, putative	-3.8
	AFUA_6G13790	monooxygenase	-3.6
	AFUA_7G02010	hypothetical protein	-3.6
	AFUA_1G07480	coproporphyrinogen III oxidase,	-3.3
	AFUA_4G08710	short chain dehydrogenase,	-3.2
Cytochrome C oxidoreductase activity P=0.008	AFUA_3G06190	Cytochrome c oxidase subunit Via	-2.6
	AFUA_3G14440	cytochrome c oxidase family	-2.6
	AFUA_2G03010	cytochrome c subunit Vb, putative	-2.5
	AFUA_5G10560	cytochrome c oxidase subunit V	-2.2

¹Top five genes with the highest fold change are shown in each category.

²Ergosterol biosynthesis pathway.

³Involvement in amino acid catabolism.

doi:10.1371/journal.pone.0033604.t001

subsequently with matrix (α -cyano-4-hydroxy-trans-cinnamic acid, Sigma). The samples were analyzed with a 5800 Proteomics Analyzer MALDI-TOF/TOF mass spectrometer (Applied Biosystems, Foster City, CA) in manual mode. All mass spectra were externally calibrated with the 4700 Proteomics Analyzer Mass Standards Kit (Applied Biosystems). Peak lists from all MS and MS/MS spectra were submitted to database search using Mascot software (www.matrixscience.com). The samples were searched against the NCBI nr database, against all taxonomies. Initial search parameters included two variable modifications: Carbamidomethyl (C) and Oxidation (M). Up to one missed cleavage site was allowed, peptide mass tolerance was 0.05 Da, and MS/MS tolerance was 0.2 Da. The accession number and the name of the ORF were taken from the Universal Protein Resource server using the database UniProt Knowledge/Swiss-Prot. The prediction of a signal peptide (SignalP) in the sequence of identified proteins was

investigated by the Fungal Secretome Knowledge Base (FunSecKB).

Results

Microarray analysis

We have previously shown that deletion of the gene encoding the *A. fumigatus* transcription factor PrtT, results in decreased transcription of secreted proteases and loss of secreted protease activity [11]. To better understand this process at the transcriptomic level, we determined changes in gene expression between *A. fumigatus* WT and *ΔprtT* strains by microarray analysis. WT or *ΔprtT* conidia were grown in SM for 24 h, harvested and RNA was extracted. SM medium was used because it induces strong protease secretion in the WT and none in the mutant [11]. There was no difference between the dry weight of the WT and *ΔprtT*

Table 2. Selected enriched upregulated gene classes in the *AprtT* mutant vs. *W.*

Enriched class	Gene ID	Gene description	Fold change
Transporter activity, GO:0005215 <i>P</i> = 0.008	AFUA_8G00540 ²	hybrid polyketide synthase/nonribosomal peptide synthase, pseurotin biosynthesis	43.1
	AFUA_8G00370 ²	polyketide synthase, putative	27.7
	AFUA_8G00940	MFS drug transporter, aflatoxin exporter	21.0
	AFUA_8G00800	amino acid transporter, putative	9.9
	AFUA_2G09860	purine-cytosine permease	8.1
	AFUA_6G11840	sodium:bile acid symporter involved in azole resistance	5.4
	AFUA_4G01230	amino acid transporter, putative	5.2
	AFUA_6G03060	MFS monosaccharide transporter	5.0
	AFUA_1G12240	MFS peptide transporter, putative	4.6
	AFUA_5G11020	ammonium transporter	4.3
Oxidoreductase activity, GO:0016491 <i>P</i> = 0.04	AFUA_8G00480 ²	phytanoyl-CoA dioxygenase family protein	41.9
	AFUA_8G00560 ²	cytochrome P450, similar to SP:P79084:O-methylsterigmatocystin oxidoreductase (<i>Aspergillus flavus</i>)	38.1
	AFUA_8G00440 ²	steroid monooxygenase, putative	15.8
	AFUA_6G11850	hypothetical protein	11.4
	AFUA_4G14780 ²	cyp5081A1 cytochrome P450 monooxygenase, putative	10.3
	AFUA_5G08900	D-arabinitol dehydrogenase ArbD, putative	9.5
	AFUA_4G14800 ²	sdr1 short chain dehydrogenase, putative	9.5
	AFUA_1G04150	tartrate dehydrogenase	8.9
	AFUA_3G12960 ²	cytochrome P450 monooxygenase (GliC ortholog), putative	8.6
	AFUA_8G00510 ²	O-methylsterigmatocystin oxidoreductase, putative	7.0

¹Top 10 genes with the highest fold change are shown in every category.

²Gene located in a gene cluster.

doi:10.1371/journal.pone.0033604.t002

strains at harvesting, suggesting that their growth rates after 24 h were similar. The 24 h time point was selected because we previously demonstrated that *prtT* mRNA levels are highest after 24 h of growth [11].

Expression of genes involved in iron uptake and ergosterol biosynthesis is significantly reduced in the *AprtT* mutant

There was at least twofold decrease in the mRNA levels of 199 genes in the *AprtT* mutant strain relative to the WT (see Supporting Information S1). These genes were categorized by the Expander program and included, as expected, genes encoding secreted proteases ($p = 0.002$), but also, surprisingly, genes involved in iron uptake ($p = 1E-15$) and in steroid and fatty acid biosynthesis ($p = 0.001$). The *AprtT* mutant also showed significantly reduced transcript levels of genes involved in cellular ketone metabolic processes ($p = 0.001$) and transcripts encoding proteins with oxidoreductase activity ($p = 0.008$) in particular cytochrome C oxidoreductase activity ($p = 0.008$) (See Table 1 and Table B in Supporting Information S2, all reported terms are after FDR correction of 0.05). Remarkably, among the downregulated genes, those involved in iron uptake showed the most dramatic decrease ($p = 1.64E-5$ using Wilcoxon rank sum test). Fig. 1 depicts the top 50 downregulated genes in ascending order. This group contains 10 genes related to iron uptake that are strongly downregulated in the *AprtT* mutant (average fold change -20, in comparison to an average of -6.2 among the 40 other genes). The results suggest that in addition to activating the transcription of secreted

proteases, PrtT may also be involved in the activation of iron-uptake genes, and in particular 8 of the 10 genes involved in non-reductive iron uptake by siderophores (*sida-G*/siderophore biosynthesis, *Sit1/MirB/MirC*-siderophore transporters) and 2 out of the 3 genes involved in reductive iron uptake (*Fre2*-secreted ferric reductase, *FtrA*-permease) [14,27]

Interestingly, 6 of the 11 genes categorized as participating in steroid and fatty acid biosynthesis and downregulated in the *AprtT* mutant are directly involved in the biosynthesis of ergosterol (hyper-geometric p -value = $1.8E-6$) including the key pathway genes ERG1, ERG3, ERG11/Cyp51A,B (Table B in Supporting Information S2, footnote 1). Also notable was the finding that 8 of the 14 genes categorized as participating in cellular ketone metabolic processes and downregulated in the *AprtT* mutant are directly involved in amino acid breakdown, possibly due to a shortage of available amino acids upon reduced protease secretion by the mutant (Table 1 and Table B in Supporting Information S2, footnote 2).

Expression of gene clusters involved in secondary metabolite biosynthesis is significantly increased in the *AprtT* mutant

There was a twofold or higher increase in the mRNA levels of 229 genes in the *AprtT* mutant strain relative to the WT (see in Supporting Information S1). These genes were categorized by the Expander program and included genes encoding transporters ($p = 0.008$) and proteins with oxidoreductase activity ($p = 0.004$) (Table 2 and Table C in Supporting Information S2). Surprising-

Table 3. Significantly enriched physical clusters

Group	Cluster	P-value	#genes	Putative function
Down regulated	9	<E-7	9	Siderophore biosynthetic cluster
Upregulated	10	<E-6	7	ETP unknown Toxin Biosynthesis Cluster
Upregulated	15	<E-5	10	Unknown
Upregulated	22	<E-3	4	Unknown
Upregulated	24	<E-15	23	Pseurotin A biosynthetic cluster

doi:10.1371/journal.pone.0033604.t003

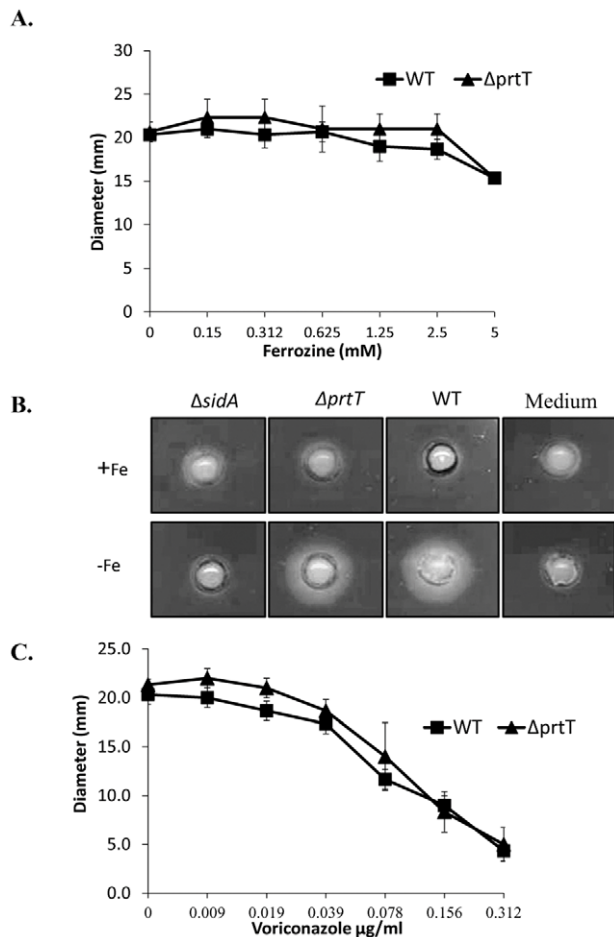


Figure 2. Phenotypic analysis of the $\Delta prtT$ mutant. (A) Growth in iron-limited media: WT and $\Delta prtT$ mutant were grown in iron-lacking 0.1% SM agar and supplemented with different concentrations of the ferrous iron chelator ferrozine. Colony diameter was measured after 48 h at 37°C. Similar results were seen with 1% SM and using liquid medium as well (data not shown). (B) Evaluation of siderophore production using the CAS assay. WT and $\Delta prtT$ conidia were grown either in liquid medium containing iron (indicated by +Fe) or on medium without iron (indicated by -Fe). Culture supernatants were collected and added to wells made in the CAS agar plates. The presence of a halo around the well indicates siderophore production. Non-inoculated growth media were also applied to wells on the CAS plate as a negative control (Medium). (C) Sensitivity to voriconazole. WT and $\Delta prtT$ mutant were grown on 1% SM agar plates supplemented with different concentrations of voriconazole. Colony diameter was measured after 48 h at 37°C.

doi:10.1371/journal.pone.0033604.g002

ly, a large number of the upregulated genes in the $\Delta prtT$ mutant are involved in secondary metabolite biosynthesis and transport ($p = 1E-15$, selected genes shown in Table 2 denoted by superscript² and Table C in Supporting Information S2, denoted by an asterisk) and some are members of gene clusters previously described in Nierman et al. [24]. We therefore identified all of the genes in our microarray dataset that were significantly up- or downregulated in the $\Delta prtT$ mutant and located in a gene cluster (Table 3 and Table D in Supporting Information S2, all accepted terms are after FDR correction of 0.05). The results showed that nine genes of siderophore biosynthetic cluster 9 were downregulated in the $\Delta prtT$ mutant relative to the WT, whereas four clusters (10, 15, 22 and 24) were upregulated. The function of clusters 10, 15 and 22 is unknown. The genes upregulated in cluster 24 are involved in pseurotin A biosynthesis (Table 3 and Table D in Supporting Information S2). These results suggest that the $\Delta prtT$ mutant may produce more secondary metabolites than the WT when grown in SM medium.

The $\Delta prtT$ mutant does not exhibit increased sensitivity to iron deprivation or to inhibition of ergosterol biosynthesis

The results of the microarray analysis, showing reduced expression of genes involved in iron uptake in the $\Delta prtT$ strain, suggested that it may be more sensitive to iron deprivation. We therefore compared the radial growth of the WT and $\Delta prtT$ strains in the presence of increasing concentrations of the ferrous iron chelator ferrozine (Fig. 2A). The $\Delta prtT$ strain was not more sensitive than the WT under iron limitation. Furthermore, the $\Delta prtT$ strain was not attenuated in its ability to secrete siderophores under iron limitation as measured by the CAS halo assay (Fig. 2B, compare halo diameters -Fe of WT and $\Delta prtT$ strain).

The results of the microarray analysis, showing reduced expression of genes involved in ergosterol biosynthesis in the $\Delta prtT$ strain, suggested that it may be more sensitive to azole antifungals which inhibit ergosterol biosynthesis. To test this possibility, we compared the radial growth of the WT and $\Delta prtT$ strains in the presence of increasing concentrations of voriconazole (Fig. 2C): again, the $\Delta prtT$ strain was not more sensitive than the WT in the presence of increasing concentrations of voriconazole.

Compensatory gene activation occurs in the $\Delta prtT$ mutant under stress

We hypothesized that the $\Delta prtT$ strain fails to show a sensitive phenotype under iron limitation or in the presence of voriconazole because of compensatory transcriptional activation of the genes involved in these pathways. We therefore used qPCR to analyze the mRNA levels of (i) *MirB* (siderophore transporter), *SidA* (siderophore synthesis) in response to iron limitation and (ii) *Erg11* (sterol demethylase), *Erg3* (sterol 5,6

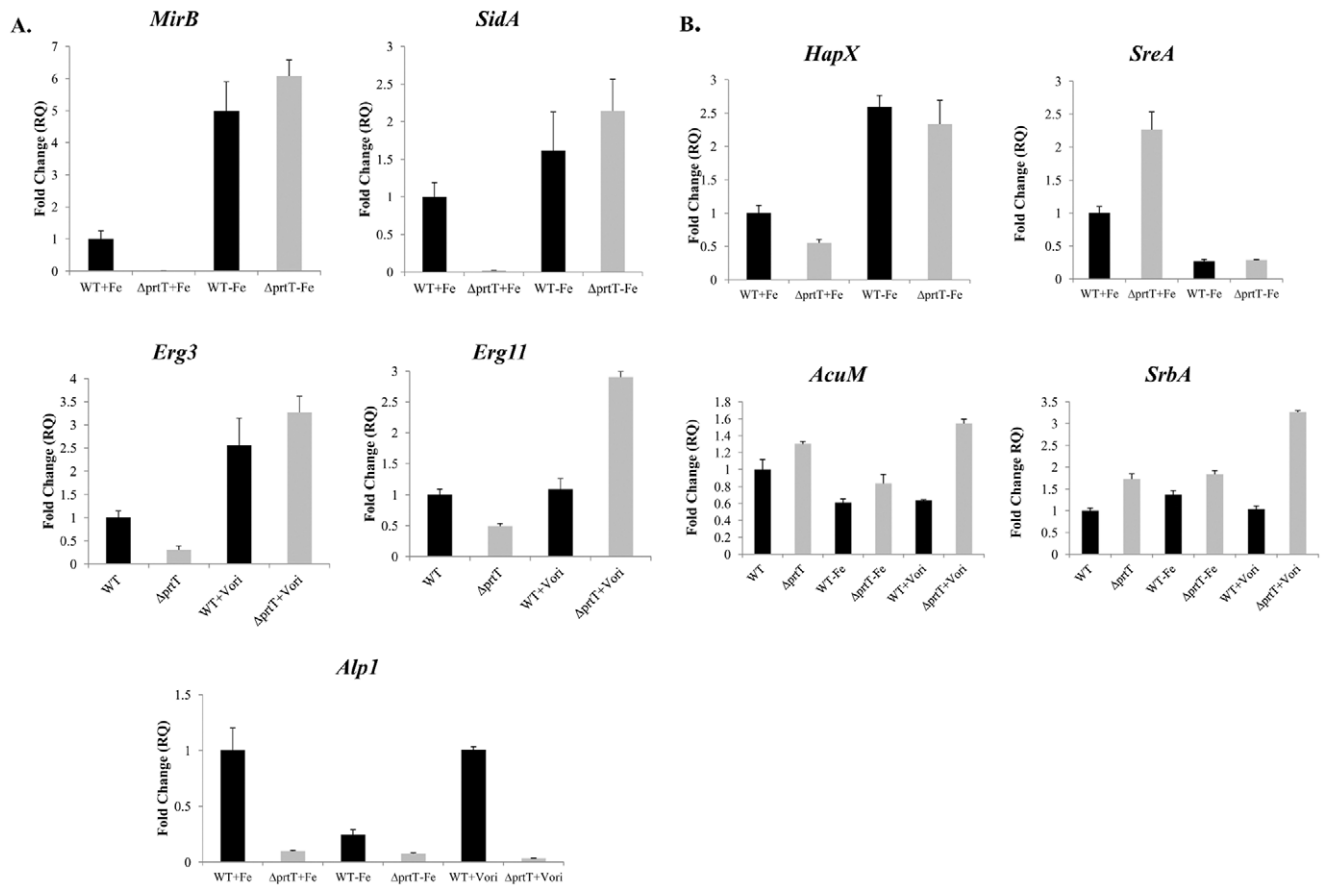


Figure 3. qRT-PCR evaluation of transcripts levels from genes that showed a differential expression in the microarray (A) representative genes (*MirB*, *SidA*, *Erg3*, *Erg11* and *Alp1*) and (B) the genes *HapX*, *SreA*, *AcuM* and *SrbA* encoding transcription factors that regulate iron uptake. Expression rates were normalized relative to mRNA levels of the β -tubulin-encoding gene (AFUA_1G10910) and set arbitrarily to 1 for the WT strain grown in 1% SM medium. Values are given in relative quantity of template compared to the original sample (RQ). RQ values were calculated by use of the equation: $RQ = 2^{-\Delta\Delta CT}$, with $\Delta\Delta CT \pm SD$ and $\Delta CT \pm SD$ s. -Fe = growth medium lacking iron and containing 1 mM ferrozine. +Vori = growth medium supplemented with a sub-inhibitory concentration (0.125 μ g/ml) of voriconazole. The experiment was repeated three times with similar results. Graphs show a representative experiment. doi:10.1371/journal.pone.0033604.g003

desaturase) in response to a sub-inhibitory concentration (0.125 μ g/ml) of voriconazole (Fig. 3A). The level of *Alp1* protease mRNA, which we have previously shown to be strongly down-regulated in the Δ prtT strain [11], was used as a control. Results showed that *MirB*, *SidA*, *Erg11*, *Erg3* and *Alp1* mRNA levels are strongly reduced in the Δ prtT strain in comparison to the WT when grown in SM liquid medium, independently validating the microarray results. However, in both WT and Δ prtT strains, *MirB*/*SidA* and *Erg11*/*Erg3* mRNA levels were strongly increased in SM medium lacking iron, or containing voriconazole, respectively (Fig. 3A). In contrast *Alp1* mRNA levels were not increased in the Δ prtT strain under these conditions (Fig. 3A). Together, these results indicate that compensatory transcriptional mechanisms activated in the Δ prtT strain under iron limitation or inhibition of ergosterol biosynthesis are responsible for the lack of increased sensitivity to these treatments compared to the WT strain. Two transcription factors, HapX (activator) and SreA (repressor) are primarily involved in regulating iron uptake [14,16]. We hypothesized that growth of the Δ prtT strain under iron limitation activates HapX and inhibits SreA expression, bypassing the need for PrtT. We therefore used q-PCR to analyze the mRNA levels of HapX and SreA in the WT and Δ prtT strain under normal and limiting iron

levels. In SM medium containing normal iron levels, the Δ prtT strain expressed reduced levels of HapX activator and increased levels of SreA repressor compared to WT (Fig. 3B). This result (decreased activator, increased repressor) might explain the observed reduced expression of iron uptake genes in this mutant. In contrast, under iron starvation, the Δ prtT strain underwent a corrective compensatory response. It expressed elevated levels of HapX and reduced levels of SreA in a manner similar to the WT (Fig. 3B). This supports our hypothesis that under iron limitation the Δ prtT strain activates HapX and inhibits SreA expression, bypassing the need for PrtT and enabling it to grow like the WT under these conditions. Recently, two additional transcription factors, *AcuM* and *SrbA* were shown to activate transcription of HapX, increasing iron uptake and ergosterol biosynthesis [17,33]. However, *AcuM* and *SrbA* mRNA levels were not altered in the Δ prtT strain compared to the WT, nor were they induced under limiting iron levels or the presence of sub-inhibitory concentrations of voriconazole (Fig. 3B). This result suggests that PrtT functions independently of *AcuM* and *SrbA*.

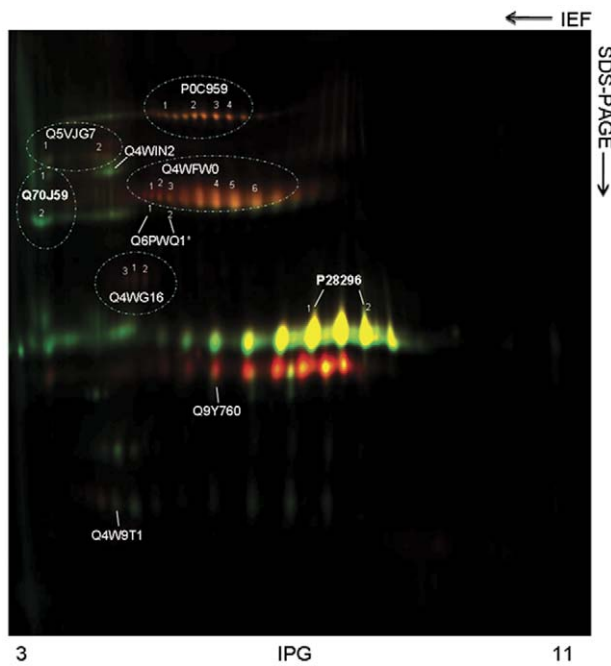


Figure 4. 2-D DIGE comparing the secretomes of WT and Δ prtT strains. DIGE image overlay of WT (Cy3 label in green) and Δ prtT (Cy5 label in red) secretomes. Yellow spots indicate proteins detected in both strains and identified proteins are indicated by their accession number (SwissProt/UniProtKB database). Detected protein isoforms are represented with Arabic numerals.
doi:10.1371/journal.pone.0033604.g004

Secretome analysis by 2D-DIGE

The proteins present in the secretome of the WT and Δ prtT strains were evaluated by a 2D-DIGE quantitative proteomic analysis, followed by MALDI-TOF/MS analysis.

The DIGE approach was used to quantify changes in protein expression of the most abundant species in both strains, because this technique shows high sensitivity for in-gel analysis of the differentially expressed proteins. This type of approach was applied because the aim was not to identify all proteins secreted but only the major differences in protein expression between the strains. The resultant gel shown in Figure 4 is representative of all five independent gels and five biologicl replicates which were used in the DeCyder analysis and the EDA mode analysis. All independent gels were imaged by scanning with different excitation wavelengths, producing protein profiles for each sample which were then overlaid, to enable exact matching of protein spots for the WT and Δ prtT secretomes (Fig. 4). Further analysis of gels using DeCyder software allows differentially expressed proteins to be accurately quantified. The 2D-DIGE analysis showed an average of 480 spots detected automatically by DeCyder software (Fig. 4). Among these, 94 spots were statistically validated using a differential abundance ratio of ≥ 1.5 -fold and $p < 0.05$. By this analysis, it was observed that the mutant strain overexpresses 63.8% of the proteins when compared with the WT. Only proteins present in at least 3 independent gels out of five, were considered to be differentially expressed. For protein identification the gels were further stained by colloidal *Coomassie* and the proteins identified as summarized in Table 4. Identified proteins are denoted by accession numbers and the protein isoform(s) are indicated by numbers (Fig. 4). All MS/MS data are presented in Table E in Supporting Information S2. In addition, the presence of signal peptides for all identified proteins was

evaluated by FunSecKB (Fungal Secretome Knowledge Base). The Δ prtT mutant expressed reduced levels of ALP1 protease, TppA tripeptidyl peptidase and AFUA_2G01250 serine peptidase and increased levels of AFU_3G00840/FAD-oxygenase, AspF chitinase, EglC endoglucanase and Bgt1 glucanoyltransferase (Table 4 and Fig. 4).

Discussion

Deletion of the *A. fumigatus* *PrtT* gene encoding a C6-zinc finger transcription factor results in decreased transcription of genes encoding six secreted proteases and subsequent loss of secreted protease activity [11,12]. To better understand the global role of PrtT in the control of gene expression and its effect on the secretome, we performed a combination of microarray and proteomics-based secretome analyses of the Δ prtT mutant.

The microarray analysis revealed several unexpected findings. First, expression of genes involved in iron uptake was dramatically decreased in the Δ prtT mutant under iron-replete (SM medium) conditions, suggesting that PrtT activates their transcription. It is unlikely that this is an indirect effect of nutrient starvation due to decreased protease secretion: SM contains sufficient glucose and amino acids and the growth rate of the Δ prtT mutant is similar to the WT in this medium. It is more likely that PrtT, in addition to activating transcription of secreted proteases, also upregulates iron uptake. Iron is needed for the activity of metalloproteases and oxidoreductases participating in the utilization of amino acids derived from protein hydrolysis. Therefore, under iron-replete conditions, PrtT positively regulates genes involved in reductive iron assimilation and siderophore-mediated iron uptake, enabling efficient utilization of proteins as an energy source. Deletion of PrtT results in the down-regulation of these genes without leading to an observable iron-dependent phenotype probably because there is enough iron available in the SM medium for low-affinity uptake to suffice. We would, however, expect the Δ prtT mutant to exhibit reduced growth under iron-depleted conditions, but as we show in this report, this is not the case. Under these conditions, transcription of genes involved in siderophore-mediated iron uptake is strongly activated, probably as a result of compensatory activation of alternative transcription factors involved in iron uptake. Indeed we show that in the Δ prtT mutant under iron starvation HapX transcript levels increase while SreA levels decrease. This would result in both direct activation (via HapX) and derepression (via reduced SreA) of genes involved in iron uptake. Iron limitation therefore appears to activate a complex hierarchy of control elements, obviating the need for PrtT activity and ensuring that the organism reacts appropriately to the environmental challenge. Our findings suggest that PrtT operates as part of a larger network of transcription factors that is wired for functional redundancy.

At present, it is not known whether PrtT directly binds to the promoters of iron-uptake genes or whether it activates their transcription by an indirect mechanism. Our in-silico promoter motif analysis failed to identify significant conserved motifs in the promoters of the down-regulated genes (our unpublished data).

A second finding of interest is that deletion of *prtT* resulted in the upregulation of four secondary metabolite clusters (10, 15, 22 and 24), suggesting that PrtT negatively regulates their activity. Whereas the functions of clusters 10, 15 and 22 are unknown, cluster 24 contains genes for the biosynthesis of fumitremorgin (AFUA_8G00170- AFUA_8G00250) and pseurotin A (AFUA_8G00530- AFUA_8G00720) [13,15,34]. Only the genes involved in pseurotin A biosynthesis were upregulated in cluster 24 in the Δ prtT mutant. Pseurotin A is a competitive inhibitor of

Table 4. Secretome proteins identified by 2D–DIGE.

Identified Protein by MS/MS	ORF	Iso-form	Accession number	MW theoretical (kDa)/pI	Signal Peptide	Expression rate-fold (Δ prtT/WT)
Secreted dipeptidyl peptidase Dpp V	AFUA_2G09030 ¹	1,2,3,4	P0C959	79.6/5.59	Y	---
Pheromone processing carboxypeptidase (Sxa2)	AFUA_2G03510	1,2	Q5VJG7	59.7/4.77	Y	---
Tripeptidyl-peptidase (TppA)	AFUA_4G03490	1	Q70J59	65.7/5.3	Y	---
Tripeptidyl-peptidase (TppA)	AFUA_4G03490	2	Q70J59	65.7/5.30	Y	-5.23
Serine peptidase	AFUA_2G01250	--	Q4WIN2	58.5/4.86	Y	-1.95
FAD-dependent oxygenase	AFUA_3G00840 ¹	1	Q4WFW0	54.9/6.52	Y	3.58
FAD-dependent oxygenase	AFUA_3G00840 ¹	2	Q4WFW0	54.9/6.52	Y	2.67
FAD-dependent oxygenase	AFUA_3G00840 ¹	3	Q4WFW0	54.9/6.52	Y	3.09
FAD-dependent oxygenase	AFUA_3G00840 ¹	4	Q4WFW0	54.9/6.52	Y	2.02
FAD-dependent oxygenase	AFUA_3G00840 ¹	5	Q4WFW0	54.9/6.52	Y	1.82
FAD-dependent oxygenase	AFUA_3G00840 ¹	6	Q4WFW0	54.9/6.52	Y	1.89
Mannosidase I	AFUA_1G14560	1	Q6PWQ1	55.4/5.14	Y	3.58
Mannosidase I	AFUA_1G14560	2	Q6PWQ1	55.4/5.14	Y	3.09
β -1,3- glucanosyltransferase Bgt1	AFUA_1G11460	1	Q4WSV9	33/5.02	Y	2.96
GPI-anchored cell wall β -1,3-endoglucanase EglC	AFUA_3G00270 ¹	1	Q4WG16	44.6/4.90	Y	2.96
GPI-anchored cell wall β -1,3-endoglucanase EglC	AFUA_3G00270 ¹	2	Q4WG16	44.6/4.90	Y	5.13
GPI-anchored cell wall β -1,3-endoglucanase EglC	AFUA_3G00270 ¹	3	Q4WG16	44.6/4.9	Y	2.75
Alkaline serine protease Alp1	AFUA_4G11800 ¹	1	P28296	42.1/6.32	Y	-3.48
Alkaline serine protease Alp1	AFUA_4G11800 ¹	2	P28296	42.1/6.32	Y	-3.46
Chitinase	AFUA_4G01290 ¹	--	Q9Y760	21.5/5.76	---	2.34
Conserved hypothetical protein	AFUA_4G03830	--	Q4W9T1	15.9/5.71	Y	4.35

¹genes also identified by Wartenberg et al. (43)
doi:10.1371/journal.pone.0033604.t004

chitin synthase and is a neuritogenic agent [35]. Its expression is elevated under stressful conditions including hypoxia, during murine lung infection and following deletion of the global secondary metabolite regulator *LaeA* and the developmental transcription factor *BrlA* [13,15,36,37]. Activation of secondary metabolite clusters in the *AprtT* mutant could be an indirect response to stress due to its inability to utilize proteins in the SM medium, or possibly a direct response resulting from interactions between *PrtT* and regulatory elements within the clusters. These possibilities remain to be examined.

The proteomic analysis identified 11 proteins secreted by the *A. fumigatus* WT strain when grown on SM medium. Of these, the *AprtT* mutant expressed reduced levels of ALP1 protease, TppA tripeptidyl peptidase and AFUA_2G01250 serine peptidase and increased levels of AFU_3G00840/FAD-oxygenase, AspF chitinase, EglC endoglucanase and Bgt1 glucanosyltransferase compared to the WT strain. The increased expression of secreted polysaccharide-degrading enzymes in the *AprtT* mutant may indicate that it is (i) undergoing more intensive cell-wall remodeling than the WT or (ii) seeking an alternative carbon source because of its inability to utilize the proteins in the SM medium as an energy source.

Several groups have analyzed the secretome of WT *A. fumigatus* grown in minimal medium [38] or in the presence of elastin, collagen, keratin [39,40] or fetal calf serum [41] as the main carbon/nitrogen source. Although there is significant variability

between the secreted proteins identified in these studies, a core group of three secreted proteases; Alp1, Mep and DppV were induced in all. The most abundant secreted proteases were Alp1 and DppV which were also identified in this study. The other three proteases identified in our study (TppA, Sxa2 and AFUA_2G01250 serine peptidase) were not identified in the other studies. Of the six non-protease secreted proteins we identified, only three (Chitinase/AFU_4G01290, EglC endoglucanase and FAD-dependent oxygenase/AFU_3G00840) were also identified by Wartenberg et al. [39]. The large variations between the different studies may be due to differences in the proteomic analysis methodology, strain backgrounds, medium composition or length of culture.

Notably, a comparison between our transcriptome and proteome datasets revealed very little correlation between them. Only ALP1 protease and AspF chitinase were significantly downregulated or upregulated, respectively, in both. Similar disparities have been shown for the yeast transcriptome and proteome datasets (Pearson correlation coefficient <0.4), and have been ascribed to post-transcriptional regulation including translational control or control of protein half life [42]. However, to measure the detailed correlation between the transcriptome and proteome of *A. fumigatus*, a parallel experiment comparing the entire proteome including all intracellular proteins to the transcriptome, needs to be performed.

The results described here may provide an intriguing explanation for why the *ΔprtT* mutant is normally virulent in a murine model of IPA, despite almost totally lacking secreted protease activity [11]. In the lungs, lacking the ability to derive nutrients from its protein-rich surroundings, the *ΔprtT* mutant may activate compensatory pathways leading, as we show in vitro, to the production of novel secondary metabolites and increased secretion of proteins not normally produced by the WT strain. These factors could raise its virulence to WT levels, despite its inability to produce secreted proteases. In fact, similar compensatory mechanisms may explain puzzling results described previously, where *A. fumigatus* mutants lacking what appear to be crucial virulence factors such as those affecting resistance to oxygen radicals [43,44] or key signaling pathways significantly affecting fungal morphology [45,46] were not decreased in virulence.

In summary, further characterization of the PrtT transcription factor showed that in addition to being primarily involved in activating the expression of secreted proteases, it is also involved in activating most of the genes for iron uptake and ergosterol biosynthesis, as well as inhibiting four secondary metabolite clusters and affecting expression of secreted polysaccharide-degrading enzymes. This study underscores the complex regulatory role and multiple redundant functions of a key fungal transcription factor.

References

- Latge JP (1999) *Aspergillus fumigatus* and aspergillosis. Clin Microbiol Rev 12: 310–350.
- Denning DW (1998) Invasive aspergillosis. Clin Infect Dis 26: 781–803; quiz 804–785.
- Latge JP (2001) The pathobiology of *Aspergillus fumigatus*. Trends Microbiol 9: 382–389.
- Brakhage AA (2005) Systemic fungal infections caused by *Aspergillus* species: epidemiology, infection process and virulence determinants. Curr Drug Targets 6: 875–886.
- Oshero N (2007) The Virulence of *Aspergillus fumigatus*. In: New Insights in Medical Mycology. Ed. Kevin Kavanagh. Springer, Dordrecht, Netherlands.
- Borger P, Koeter GH, Timmerman JA, Vellenga E, Tomee JF, et al. (1999) Proteases from *Aspergillus fumigatus* induce interleukin (IL)-6 and IL-8 production in airway epithelial cell lines by transcriptional mechanisms. J Infect Dis 180: 1267–1274.
- Kogan TV, Jadoun J, Mittelman L, Hirschberg K, Oshero N (2004) Involvement of secreted *Aspergillus fumigatus* proteases in disruption of the actin fiber cytoskeleton and loss of focal adhesion sites in infected A549 lung pneumocytes. J Infect Dis 189: 1965–1973.
- Behnsen J, Lessing F, Schindler S, Wartenberg D, Jacobsen ID, et al. (2010) Secreted *Aspergillus fumigatus* protease Alp1 degrades human complement proteins C3, C4, and C5. Infect Immun 78: 3585–3594.
- Rambach G, Dum D, Mohsenipour I, Hagleitner M, Wurznner R, et al. (2010) Secretion of a fungal protease represents a complement evasion mechanism in cerebral aspergillosis. Mol Immunol 47: 1438–1449.
- Sharon H, Amar D, Levdansky E, Mircus G, Shadkchan Y, et al. (2011) PrtT-regulated proteins secreted by *Aspergillus fumigatus* activate MAPK signaling in exposed A549 lung cells leading to necrotic cell death. PLoS One 6: e17509.
- Sharon H, Hagag S, Oshero N (2009) Transcription factor PrtT controls expression of multiple secreted proteases in the human pathogenic mold *Aspergillus fumigatus*. Infect Immun 77: 4051–4060.
- Bergmann A, Hartmann T, Cairns T, Bignell EM, Krappmann S (2009) A regulator of *Aspergillus fumigatus* extracellular proteolytic activity is dispensable for virulence. Infect Immun 77: 4041–4050.
- Perrin RM, Fedorova ND, Bok JW, Cramer RA, Wortman JR, et al. (2007) Transcriptional regulation of chemical diversity in *Aspergillus fumigatus* by LaeA. PLoS Pathog 3: e50.
- Schrettl M, Kim HS, Eisendle M, Kragl C, Nierman WC, et al. (2008) SteA-mediated iron regulation in *Aspergillus fumigatus*. Mol Microbiol 70: 27–43.
- Tsumasi-Boateng K, Yu Y, Chen D, Gravelat FN, Nierman WC, et al. (2009) Transcriptional profiling identifies a role for BrlA in the response to nitrogen depletion and for StaA in the regulation of secondary metabolite clusters in *Aspergillus fumigatus*. Eukaryot Cell 8: 104–115.
- Schrettl M, Beckmann N, Varga J, Heinekamp T, Jacobsen ID, et al. (2010) HapX-mediated adaptation to iron starvation is crucial for virulence of *Aspergillus fumigatus*. PLoS Pathog 6.

Supporting Information

Supporting Information S1 Genes up or down-regulated in the *ΔprtT* mutant strain relative to the WT. (XLSX)

Supporting Information S2 Supplemental Tables A-E. Table A. Oligonucleotides used in this study. Table B. Selected enriched downregulated genes classes in the *ΔprtT* mutant vs. WT, genes that appear in more than one class are shown in the most specific class. Table C. Selected Enriched upregulated genes classes in the *ΔprtT* mutant vs. WT. Table D. Significantly enriched physical gene clusters upregulated or downregulated in the *ΔprtT* mutant vs. WT. Table E. Identified proteins and peptides by 2D-DIGE MS/MS. (DOC)

Acknowledgments

We would like to thank Hubertus Haas for providing us with the *sidA* null strain. L.M.L.B. is a research fellow of CNPq and FAPERJ (Brazil).

Author Contributions

Conceived and designed the experiments: SH PKB GN WN DA WN IS RS LLB NO. Performed the experiments: SH PKB GN WN. Analyzed the data: SH PKB DA IS RS LLB NO. Contributed reagents/materials/analysis tools: WN RS LLB NO. Wrote the paper: SH LLB NO. Headed the research: NO. Coordinated the tasks: NO.

- Liu H, Gravelat FN, Chiang LY, Chen D, Vanier G, et al. (2010) *Aspergillus fumigatus* *AcuM* regulates both iron acquisition and gluconeogenesis. Mol Microbiol 78: 1038–1054.
- Willger SD, Puttikamonkul S, Kim KH, Burritt JB, Grahl N, et al. (2008) A sterol-regulatory element binding protein is required for cell polarity, hypoxia adaptation, azole drug resistance, and virulence in *Aspergillus fumigatus*. PLoS Pathog 4: e1000200.
- Soriano FM, Malavazi I, Savoldi M, Espeso E, Dinamarco TM, et al. (2010) Identification of possible targets of the *Aspergillus fumigatus* CRZ1 homologue, CrzA. BMC Microbiol 10: 12.
- Lessing F, Kniemeyer O, Wozniok I, Loeffler J, Kurzai O, et al. (2007) The *Aspergillus fumigatus* transcriptional regulator AfYap1 represents the major regulator for defense against reactive oxygen intermediates but is dispensable for pathogenicity in an intranasal mouse infection model. Eukaryot Cell 6: 2290–2302.
- Schrettl M, Bignell E, Kragl C, Joechl C, Rogers T, et al. (2004) Siderophore biosynthesis but not reductive iron assimilation is essential for *Aspergillus fumigatus* virulence. J Exp Med 200: 1213–1219.
- Bainbridge BW (1971) Macromolecular composition and nuclear division during spore germination in *Aspergillus nidulans*. J Gen Microbiol 66: 319–325.
- Lee CY, Cheng MF, Yu MS, Pan MJ (2002) Purification and characterization of a putative virulence factor, serine protease, from *Vibrio parahaemolyticus*. FEMS Microbiol Lett 209: 31–37.
- Nierman WC, Pain A, Anderson MJ, Wortman JR, Kim HS, et al. (2005) Genomic sequence of the pathogenic and allergenic filamentous fungus *Aspergillus fumigatus*. Nature 438: 1151–1156.
- Ulitsky I, Maron-Katz A, Shavit S, Sagir D, Linhart C, et al. (2010) Expander: from expression microarrays to networks and functions. Nat Protoc 5: 303–322.
- Monod M, Capoccia S, Lechenne B, Zaugg C, Holdom M, et al. (2002) Secreted proteases from pathogenic fungi. Int J Med Microbiol 292: 405–419.
- Kornitzer D (2009) Fungal mechanisms for host iron acquisition. Curr Opin Microbiol 12: 377–383.
- Montano SP CM, Fingermer I, Pierce M, Vershon AK, Georgiadis MM (2002) Crystal structure of the DNA-binding domain from Ndt80, a transcriptional activator required for meiosis in yeast. Proc Natl Acad Sci U S A 99: 14041–14046.
- Schwyn B, Neilands JB (1987) Universal chemical assay for the detection and determination of siderophores. Anal Biochem 160: 47–56.
- Power T, Ortoneda M, Morrissey JP, Dobson AD (2006) Differential expression of genes involved in iron metabolism in *Aspergillus fumigatus*. Int Microbiol 9: 281–287.
- Pardo M, Ward M, Bains S, Molina M, Blackstock W, et al. (2000) A proteomic approach for the study of *Saccharomyces cerevisiae* cell wall biogenesis. Electrophoresis 21: 3396–3410.

32. Pitarch A, Sanchez M, Nombela C, Gil C (2002) Sequential fractionation and two-dimensional gel analysis unravels the complexity of the dimorphic fungus *Candida albicans* cell wall proteome. *Mol Cell Proteomics* 1: 967–982.
33. Blatzer M, Barker BM, Willger SD, Beckmann N, Blosser SJ, et al. (2011) SREBP coordinates iron and ergosterol homeostasis to mediate triazole drug and hypoxia responses in the human fungal pathogen *Aspergillus fumigatus*. *PLoS Genet* 7: e1002374.
34. Maiya S, Grundmann A, Li X, Li SM, Turner G (2007) Identification of a hybrid PKS/NRPS required for pseurotin A biosynthesis in the human pathogen *Aspergillus fumigatus*. *Chembiochem* 8: 1736–1743.
35. Komagata D, Fujita S, Yamashita N, Saito S, Morino T (1996) Novel neuritogenic activities of pseurotin A and penicillic acid. *J Antibiot (Tokyo)* 49: 958–959.
36. Vodisch M, Scherlach K, Winkler R, Hertweck C, Braun HP, et al. (2011) Analysis of the *Aspergillus fumigatus* proteome reveals metabolic changes and the activation of the pseurotin A biosynthesis gene cluster in response to hypoxia. *J Proteome Res* 10: 2508–2524.
37. McDonagh A, Fedorova ND, Crabtree J, Yu Y, Kim S, et al. (2008) Subtelomere directed gene expression during initiation of invasive aspergillosis. *PLoS Pathog* 4: e1000154.
38. Schwienbacher M, Weig M, Thies S, Regula JT, Heesemann J, et al. (2005) Analysis of the major proteins secreted by the human opportunistic pathogen *Aspergillus fumigatus* under in vitro conditions. *Med Mycol* 43: 623–630.
39. Wartenberg D, Lapp K, Jacobsen ID, Dahse HM, Knimeyer O, et al. (2011) Secretome analysis of *Aspergillus fumigatus* reveals Asp-hemolysin as a major secreted protein. *Int J Med Microbiol*.
40. Sriranganadane D, Waridel P, Salamin K, Reichard U, Grouzmann E, et al. (2010) *Aspergillus* protein degradation pathways with different secreted protease sets at neutral and acidic pH. *J Proteome Res* 9: 3511–3519.
41. Neustadt M, Costina V, Kupfahl C, Buchheidt D, Eckerskorn C, et al. (2009) Characterization and identification of proteases secreted by *Aspergillus fumigatus* using free flow electrophoresis and MS. *Electrophoresis* 30: 2142–2150.
42. Gygi SP, Rochon Y, Franz BR, Aebersold R (1999) Correlation between protein and mRNA abundance in yeast. *Mol Cell Biol* 19: 1720–1730.
43. Lambou K, Lamarre C, Beau R, Dufour N, Latge JP (2010) Functional analysis of the superoxide dismutase family in *Aspergillus fumigatus*. *Mol Microbiol* 75: 910–923.
44. Lamarre C, Ibrahim-Granet O, Du C, Calderone R, Latge JP (2007) Characterization of the SKN7 ortholog of *Aspergillus fumigatus*. *Fungal Genet Biol* 44: 682–690.
45. Valiante V, Heinekamp T, Jain R, Hartl A, Brakhage AA (2008) The mitogen-activated protein kinase MpkA of *Aspergillus fumigatus* regulates cell wall signaling and oxidative stress response. *Fungal Genet Biol* 45: 618–627.
46. Jain R, Valiante V, Remme N, Docimo T, Heinekamp T, et al. (2011) The MAP kinase MpkA controls cell wall integrity, oxidative stress response, gliotoxin production and iron adaptation in *Aspergillus fumigatus*. *Mol Microbiol* 82: 39–53.